Computational Study of Redox Active Centers of Blue Copper Proteins: A Computational DFT Study

Matej Pavelka, J.V. Burda

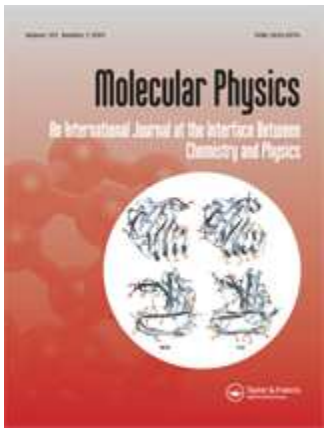

Computational Study of Redox Active Centers of Blue Copper Proteins: A Computational DFT Study

Journal:	*Molecular Physics*
Manuscript ID:	TMPH-2008-0332.R1
Manuscript Type:	Full Paper
Date Submitted by the Author:	07-Dec-2008
Complete List of Authors:	Pavelka, Matej; Charles University, Chemical Physics and Optics Burda, J.V.; Charles University, Czech Republic, Department of Chemical physics and optics
Keywords:	DFT calculations, plastocyanin, blue copper proteins, copper complexes

Computational Study of Redox Active Centers of Blue Copper Proteins: A Computational DFT Study

Matěj Pavelka and Jaroslav V. Burda*

Department of Chemical Physics and Optics, Faculty of Mathematics and Physics, Charles University, Ke Karlovu 3, 121 16 Prague 2, Czech Republic

*Corresponding author, e-mail: burda@karlov.mff.cuni.cz

Abstract

Active sites of blue copper proteins in both reduced and oxidized states were studied at the Density Functional Theory (DFT) level. Two families of these redox sites were examined: the Type A centers with methionine ligand as 4th residue and the Type B with Glutamine residue. Constrained and full optimizations were performed on the protein data bank structures in vacuo and in implicit solvent model simulating protein and water environments. It was found that the redox sites do not possess optimum geometries regardless of the oxidation state. The axial Cu-ligand bond elongates/shortens in the fully optimized Cu(I)/Cu(II) complexes. The reduced centers have a tendency to decrease the coordination number, while a trend to form four "equivalent" bonds is preferred in the oxidized centers. Comparison of the full and constrained optimizations also revealed that the A centers exhibit lower relaxation energies. In the constrained structures, a higher ionization potential was predicted for the A centers when compared to the B centers regardless of the influence of environment. The calculated relative difference of the redox potentials between various A and B centers is in good agreement with the experimental data. In the fully optimized complexes, the redox properties are dependent on the environment but

usually higher IP for the B centers is predicted. Partial charges, MO's, and spin density distributions (obtained by natural population analysis) were analyzed together with calculated electron paramagnetic resonance (EPR) spectra for deeper understanding of the obtained results.

1. Introduction

Every sixth entry in the protein data bank (PDB) contains a metal cofactor. Such statistics demonstrate the importance of the metal ions for catalytic processes in a living cell. Hence, investigation of metal sites – such as copper redox centers – is essential for determination of molecular mechanisms in biochemistry. The Cu ions often exhibit interesting spectral properties, which originate from the unusual geometric and electronic structures that are imposed through their interactions with protein environment. Such proteins provide many functions: electron transfer, oxidation-reduction processes, oxygen transport and insertion, and so forth.

Blue copper proteins forms the so-called Type 1 Cu proteins[1,2]. These Cu proteins have an intense absorption band near 600 nm in the oxidized Cu(II) state. This transition is assigned with the S(cysteine)-Cu Ligand-to-Metal-Charge-Transfer (LMCT). Structures of the active sites usually contain a 4-coordinated Cu ion, though a coordination number of five was found in azurins. Structural motif consists of the arrangement Cu(I)/Cu(II):(His)2CysX, where X is Met or Gln. Examples of this motif can be found in pseudoazurin, rusticyanin, plastocyanin, mavicyanin, auracyanin, stellacyanin, umecyanin, and amicyanin. Interestingly, reduction of the Cu(II) ion to Cu(I) in type 1 proteins causes minimal structural changes. It results in a low activation barrier for the Cu(I)→Cu(II) redox process and thus a rapid electron

transfer. Very interesting review on these complexes was published recently by Solomon[3].

There is a large number of works investigating biological activity of the copper proteins using both experimental and theoretical approaches. By means of UV-VIS and EPR spectroscopy, Cu-center of azurin was studied[4]. Spectroscopic tools in combination with DFT calculations were used to investigate the role of amino acid in axial position to the copper complex and its influence on a reduction potential[5]. Published experimental works include a vast range of techniques, e.g. fluorescence spectroscopy[6], X-ray absorption near-edge structure (XANES) spectra[7][8], combination of EPR and electron-nuclear double resonance (ENDOR) techniques[9], EPR and UV-VIS spectra[10], and many other. The basic aspects of a copper coordination in the protein environment are summarized in reviews[11-14]. Charge transfer (CT) dynamics of the blue copper proteins was investigated using a pump-probe[15] and resonance Raman spectroscopy[16]. Some other experimental studies dealing with these proteins should be also mentioned[17-19]. Theoretical studies of the copper interactions with amino acids have been reported recently[20-30]. A lot of computational effort was devoted to the examination of copper proteins[31-40]. The first theoretical spectra of plastocyanin were computed by Solomon's group[41,42] and many studies were reported recently, e.g.[43-49]. Calculation of the EPR parameters were published for aqua-ligated Cu(II) complexes at the modified B3LYP level[50]. Similarly also azurin and some other blue copper proteins were explored[51]. In the case of plastocyanin, QM/MM method was successfully applied[43]. Force-field potentials were developed for Cu-ligand interactions in plastocyanin[52] and applied in the study of LMCT dynamics for this protein[53]. An analogous attempt to construct an empirical force-field for the oxidized form of blue

copper proteins was made earlier based on DFT calculations[54]. Same authors studied coordination bonds in amicyanin and rusticyanin using QM/MM (IMOMM) method[55].

A great attention was also paid to examination of the "small inorganic complexes" in order to determine coordination geometries and electronic properties of various copper compounds. Investigation of these small models can provide a deeper insight into and an easier interpretation of the Cu(I)/Cu(II) behavior. Interactions of the both Cu cations with molecules like water, ammonia, or hydrogen-sulfide were intensively studied by many researchers[56-76]. A more detailed literature discussion on this topics can be found in our previous papers where these complexes were inspected[77-79].

This study focuses on models of active mononuclear centers, which are present in blue copper proteins (e.g. plastocyanin in ***Figure 1***). This study gives a comparison of electronic properties for general tetra-coordinated complexes with the active centers of blue copper proteins (within the fixed-geometry from pdb structures).

2. Computational Details

Active sites of the blue copper proteins (***Scheme 1***) were studied at the DFT level of theory. In the Type A family of the blue proteins (with Met residue), the following protein structures from the PDB database[80] were considered: amicyanin (1AAC), auracyanin (1QHQ), plastocyanin (1KDI and 1KDJ), and rusticyanin (1A3Z and 1RCY). In the case of the Type B centers (with Gln residue), the following proteins were analyzed: mavicyanin (1WS8), stellacyanin (1JER), and umecyanin (1X9R and 1X9U). These X-ray crystal structures were obtained with resolution in range from

1.33 to 1.90 Å. Structures of azurin were omitted, since they contain the second axial ligand forming 5-coordinated copper center. This study concerns only 4-coordinated redox centers, where the Cu(I)/Cu(II) cation (***Scheme 1***) is coordinated with: cysteine, two histidines, and methionine (A centers) or glutamine (B centers).

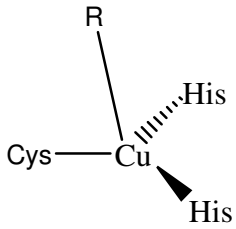

Scheme 1: The 4-coordinated Cu(I)/Cu(II) redox center of blue copper proteins. Residue R is either methionine or glutamine.

In the present work, histidine residues were modeled by imidazol, cysteine by the negatively charged methyl-thiolate $[S(CH_3)]^{1-}$, methionine by dimethyl-sulfide $S(CH_3)_2$, and glutamine by acetylamine $OC(CH_3)(NH_2)$. These models are illustrated in ***Figure 2***.

Structure optimizations were performed at several levels. In the first step (labeled "Constrained optimization"), the PDB structures are used as starting geometries. The Cu-ligand distances as well as orientation of ligands were kept frozen as shown on ***Scheme 2a***. This way, the Cu-L distances and bonding directions (Cu

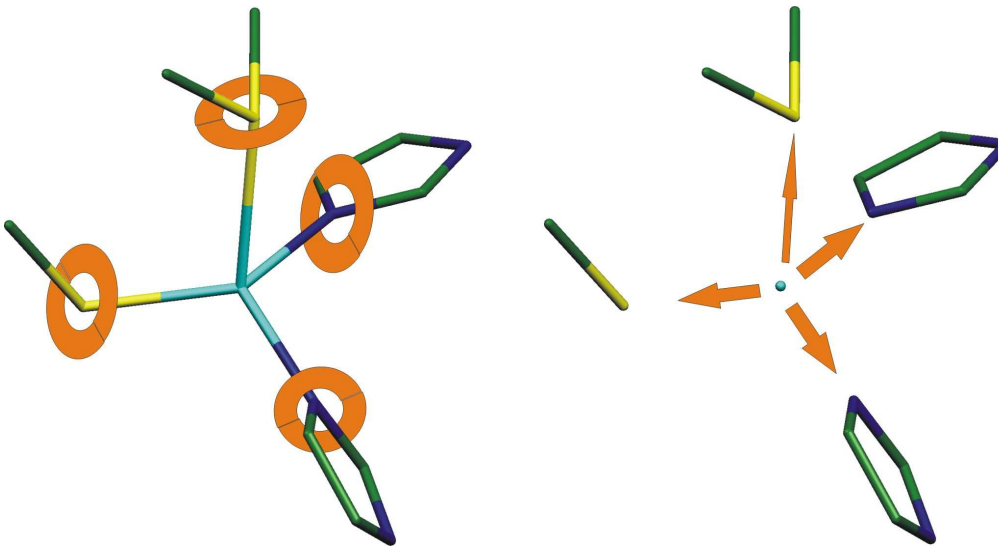

a) ***b)***

Scheme 2: Constrained optimizations: ***a)*** phase I ***b)*** phase II.

valence angles) of amino acids remain unchanged.

During the second optimization step (labeled "Constrain optimization phase II"), the copper cations could move freely (***Scheme 2b***) in the fixed framework of frozen ligands (resulting from the previous optimization phase). In the last step, the full optimization of the whole complex was allowed leading to the reduction of all the Type A centers to one final structure and analogous reduction also occurred in the case of the B centers. Since the second optimization step did not bring any important changes in coordination, it is not considered in further text.

Quantum chemical calculations were performed at the DFT level using the B3LYP functional. For the H, C, O, N atoms, the *6-31+G(d)* basis set was applied. The copper core electrons were described by the Christiansen Averaged Relativistic Effective Pseudopotentials (AREP)[81]. A consistent basis set was adopted for the valence electrons. Double-ζ pseudoorbitals of Cu were augmented by the diffuse and polarization functions (α_s = 0.025, α_p = 0.35, α_d = 0.07, and α_f = 3.75). Similarly, pseudoorbitals of the sulfur atom were extended by analogous functions with exponents: α_s = 0.077, α_p = 0.015, and α_d = 0.50.

Reduced centers with the Cu^+ cation were represented by a closed shell singlet electronic ground state, while the oxidized Cu(II) complexes, where $3d^9$ electron configuration is present, possess doublet ground states. Hence, some attention had to be devoted to the correct initial guess for the SCF procedure and the appropriate character of the wave function was checked in the end of every calculation.

All optimizations were preformed in vacuo as well as with inclusion of the solvation effects. The Conductor-like screening model (COSMO)[82,83] was used to simulate two environments: water (with relative permittivity ε = 78) and protein-like environment (ε = 4).

Having obtained the optimized structures, further analyses were performed at the higher computational level. More accurate *6-311++G(2df,2pd)* basis set was used for the H, C, N, and O atoms. At this level, the Stuttgart ECP pseudopotentials were used for both the Cu and S atoms. The basis sets on the copper/sulfur atoms were consistently enlarged by *spd/sp* diffuse functions and *2fg/2df* polarization functions ($\alpha_f = 1.00, 0.26, \alpha_g = 0.66/ \alpha_d = 0.92, 0.29, \alpha_f = 0.57$).

Energy analysis consists of evaluation of stabilization ΔE^{Stab} and bond ΔE^{BE} energies. In these calculations, Basis Set Superposition Error (BSSE) corrections and corrections on the deformation energies[84] were considered according to the equation

eq. (1) $$\Delta E^{Stab} = -(E_{complex} - \sum E_{fragment}^{BSSE} - \sum E^{deform})$$

where $E_{complex}$ represents the total energy of the whole complex and $E_{fragment}^{BSSE}$

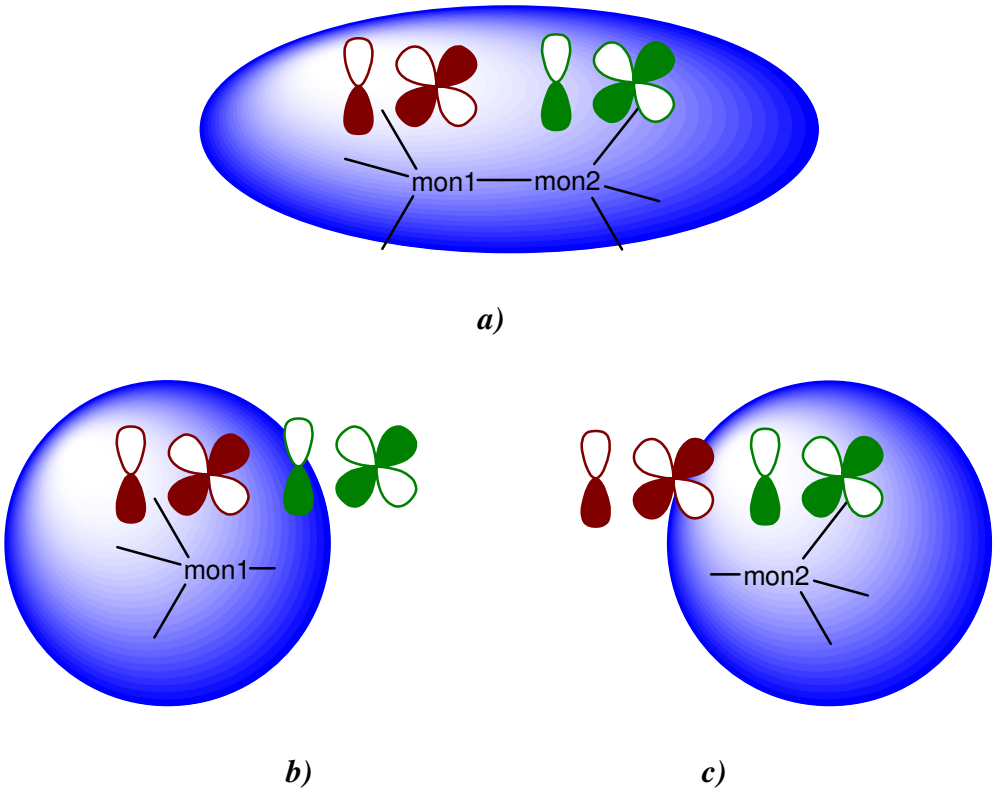

Scheme 3: Construction of boundary between the continuum and the solute within the BSSE scheme. In equation **(1)**, ***a)*** represents $E_{complex}$, while ***b)*** and ***c)*** illustrate estimations of the $E_{fragment}^{BSSE}$ energies.

represents the energy of a given subsystem computed with basis functions on the ghost atoms from the complementary part(s) of the system. Deformation energy is a sum of energy differences where for each fragment energy of fully optimized structure and energy of frozen geometry taken from the whole complex are subtracted ($E^{deform} = \sum_{fragments} (E^{optim} - E^{frozen})$, using the same number of basis functions for each fragment). In case of the BSSE calculations within the COSMO model, it is not clear how to estimate the $E^{BSSE}_{fragment}$ energies. In the present work, we propose location of the solvation cavity only around the monomer (***Scheme 3***), regardless the fact that the basis functions on the ghost atoms are located outside the cavity. In this computational scheme, it is necessary to replace values of the dispersion and repulsion energies, since inclusion of the ghost functions in the BSSE calculations of $E^{BSSE}_{fragment}$ leads to incorrect values of these energies. The correct dispersion and repulsion terms were taken from the single-point calculations of the corresponding deformation corrections (for further details see ref. [85]).

In addition, total coordination energies (ΔE^{TCE}) were also determined. In this case only two fragments were considered in eq. (1): a) all the interacting ligand molecules treated as one subsystem and b) the central Cu ion as another one. These values can be understood as the binding energies of the cation with a pre-formed ligand shell. In our previous work[77-79], the ΔE^{TCE} energies were labeled ΔE^{Stex}. The difference between ΔE^{Stab} and ΔE^{TCE} estimates the energy, which must be invested to form the ligand shell arrangement in the absence of the ion. However, the actual interligand repulsion is larger in the presence of the cation due to the additional polarization effects[86].

The ΔE^{BE} energies of the Cu-L ligand bonds were obtained using eq. (1) where partitioning according to Cu-L bond must be used. The ΔE^{BE} values were considered without the contributions of the deformation corrections.

In order to describe redox activity of the studied complexes, vertical and adiabatic ionization potentials (IP) were calculated for the reduced Cu(I) centers according to formula:

(2) $$IP = E_{Cu(II)} - E_{Cu(I)}.$$

In the case of the vertical IP, the $E_{Cu(II)}$ term represents the energy of a (2+) charged system calculated in the Cu(I) optimized structure. For the adiabatic IP, the $E_{Cu(II)}$ energy was determined from the Cu(II) optimized structure.

The charge and spin distributions were analyzed in terms of partial atomic charges and spin densities were obtained by the Natural Population Analyses (NPA)[87]. Spin isodensities (ρ_s = 0.01e/Å^3) were plotted together with selected Molecular Orbitals (MO).

Main axes of a diagonalized g-tensor were estimated in order to investigate the EPR spectrum and consequently the behavior of the unpaired electron for all studied Cu(II) complexes.

All the quantum chemical calculations were performed using *Gaussian 03* program package[88]. NBO v. 5.0 program from Wisconsin University[89] was used to evaluate the Natural Bond Orbital (NBO) characteristics and AIMPAC program was used Bader's AIM[90] (Atoms in Molecules) analyses . For visualization of geometries, spin densities, and molecular orbitals, graphical programs Molden v. 4.4[91] and Molekel v. 4.3[92,93] were used.

3. Results and Discussion

3.1 Structures

Structures of both oxidized and reduced centers of the A and B Types (see ***Figure 2***) of blue copper proteins were optimized in consequent steps with selected coordinates frozen in order to enlighten the role of the protein constraints.

3.1.1 Protein structures – Constrained optimizations

The averaged coordination distances for the oxidized Cu(II) centers of the both Types are compiled in ***Table 1***. Bond lengths obtained from the constrained optimizations correspond directly to the PDB distances from the X-ray structures.

In average, the Cu(II)-S(cysteine) bonds are about 2.2 Å long. For a comparison, the Cu-X (S, O, N) distances (in Å) for $[Cu(H_2S)_m(H_2O)_n(NH_3)_k]^{2+/+}$ cations from our previous study[79] are presented in ***Table 2*** together with values obtained from the CSD database by Katz et al.[23]. Significantly longer Cu(II)-S distances (about 2.4 Å) were found in the 4-coordinated complexes with electro-neutral H_2S ligands. In the models of blue copper proteins, the shorter Cu-S(Cys) bond can be explained by a stronger enhancement of the dative bond by electrostatic interaction between the Cu^{2+} cation and the present Cys model (thiolate $[S(CH_3)]^{1-}$). In the case of Met model (thioether group $S(CH_3)_2$), only a weaker monopole-dipole (μ = 1.6 D) interaction is present. This fact correlates with the visibly longer Cu-S(Met) bond (ca 2.89 Å). Glutamine exhibits coordination distances of about 2.15 Å. It is caused by smaller radii of the oxygen atom (in comparison with more diffuse sulfur) and by a larger dipole moment (μ = 4.0 D) of the acetyl-amine group. Corresponding bond lengths of the Cu(II) aqua complexes from our previous study[79] were determined to amount in average to 2.01 Å. The difference can be partially explained by the forced geometry of the protein centers, where the axial position of the 4^{th} ligand is disfavored (cf. below).

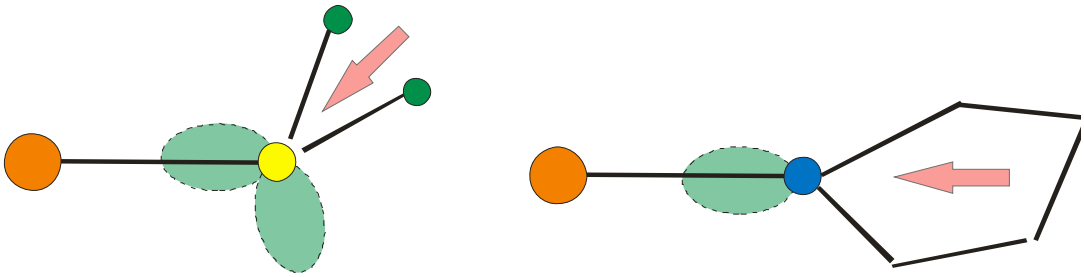

a) *b)*

Scheme 4: Metal-ligand arrangements for ***a)*** methionine and ***b)*** histidine molecules. Dashed ellipses represent lone pairs of ligands, while arrows stand for dipole orientations.

Orientation of the ligand is a result of a competition of electrostatic and dative interactions between metal and donating lone pairs of ligand molecules. According to ***Scheme 4a***, ligands with oxygen and sulfur atoms usually do not have dipole moment oriented in the direction of Cu-L bond. On the contrary, histidine has a more pronounced dipole moment nearly collinear with direction of the donated electron lone pair (and Cu-N bond). This is one of the reasons why the two Cu-N(His) distances are relatively short, about 1.97 and 2.04 Å long. These bond lengths are in good agreement with our previous results for the ammine complexes (cf. ***Table 2***).

The frozen PDB Cu-L coordination distances and the L_1-Cu-L_2 valence angles represent an influence of the protein structure. The X-ray crystal structures of blue copper proteins have a S(Cys) atom and two N(His) atoms arranged in a triangle with central metal atom placed about 0.5 Å above this plane. The 4^{th} residue is located in axial position, which is further modified by the oxidation state of the redox center.

The Cu(I)-ligand bond lengths of the reduced copper centers are presented in the second part of ***Table 1***. The Cu(I)-L (L=S, N) distances undergo only slight changes in the oxidation/reduction process of the centers. A certain elongation of Cu-O coordination bond occurs in the reduced complexes with glutamine (2.28 Å). It

should be stressed that an asymmetrical arrangement of the two Cu-N(His) distances is apparent in the PDB structures.

When oxidation state is altered, the redox centers of blue copper proteins exhibit small changes in the copper-ligand distances, meaning that qualitatively the same geometry is conserved. This can be considered to be a consequence of the protein "matrix". For the previously studied[79] 4-coordinated inorganic copper complexes, transition from the Cu(II) to Cu(I) states is connected with pronounced structural changes from square-planar to tetrahedral ligand arrangements. When such systems are allowed to be even more relaxed, they transform to 2-coordinated structures as illustrated in ***Figure 3***. This fact is important especially for the electron transferring proteins. Small structural changes of the active centers – basically changes of the Cu-L(Met/Gln) distances – minimize the reorganization energy λ within the redox process, and thus enable a rapid electron transfer.

3.1.2 Fully optimized structures in vacuo

When the models of reduced centers are optimized without any restrictions in vacuo, interesting changes can be noticed (see ***Figures 4a*** and ***4b***). The Cu atom, which lies above S, N, N-plane in non-optimized Cu(I) structures, moves so that it is situated within this plane. In the Type B center, two additional H-bonds are formed between the carbonyl group and histidines (d(O..H(His)) = 2.16 and 2.41 Å). Substantially weaker hydrogen bonding [d(S(Met)..H(His)) = 2.96 Å and d(S(Cys)..H(His)) = 3.07 Å] is surmised in the Type A center, too.

Coordination distances of the fully optimized Cu(I) complexes are presented in ***Table 1***. While the thiolate Cu-S(Cys) bond remains practically unchanged, the thioether Cu-S(Met) and carbonyl Cu-O(Gln) bonds elongate to 4.4 and 3.7 Å, respectively. The difference between the Cu-N(His1) and Cu-N(His2) distances

becomes more pronounced in the fully optimized Cu(I) complexes. Moreover in the case of the Type A center, the S-Cu-N angle between Cu-S(Cys) and the shorter of Cu-N(His) bonds opens from 131˚ (in average) to 151˚. These features (illustrated in ***Scheme 5a***) lead to an assumption that reduced centers without protein constraints would have a tendency to lower the coordination number (cf. similar trend in bond energies bellow). This finding is in accord with our previous work, where the Cu(I)/Cu(II) cations in the hydrogen sulfide-aqua-ammine ligand fields were investigated. It was shown that the "small" Cu(I) complexes with O- and N-ligands favor 2-coordinated structures[78], while the complexes with S-ligands usually prefer 3-coordination[79].

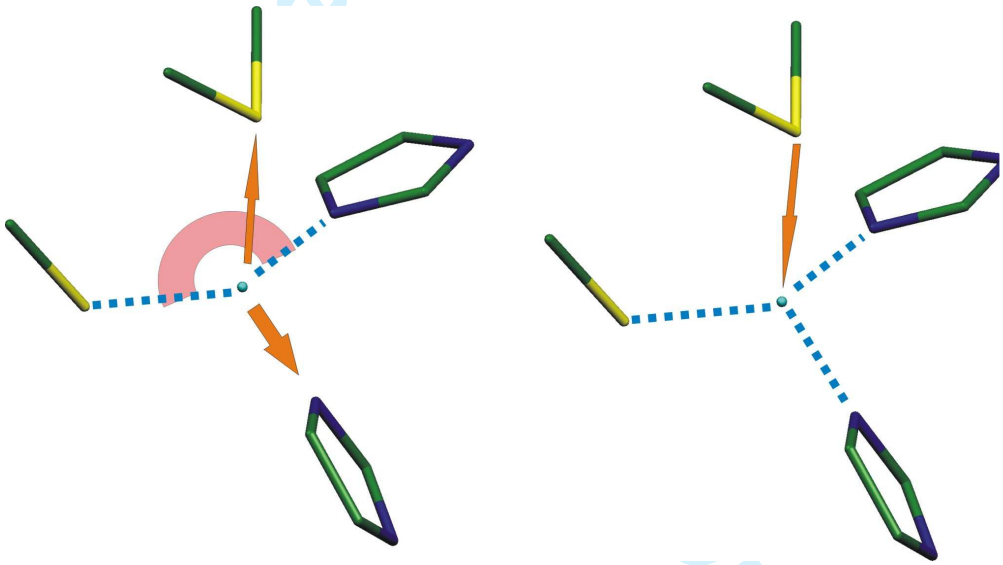

a) ***b)***

Scheme 5: Type A centers: an illustration of changes when passing from PDB structures to fully optimized geometries in vacuo.

a) reduced Cu(I) ***b)*** oxidized Cu(II) centers.

The fully optimized models of the oxidized Cu(II) centers in vacuo revealed an opposite trend. The difference between two Cu(II)-N(His) distances diminishes, especially for the Type A centers. Both the thioether Cu-S and carbonyl Cu-O bonds

are visibly shortened. Therefore, formation of oxidized centers with 4-coordination geometry is favored; the same trend is confirmed from the bond energies below. The 4-coordination is also preferred for the inorganic $[Cu(H_2S)_m(H_2O)_n(NH_3)_k]^{2+}$ complexes[79].

The full optimization has marginal effect on the Cu-S(Cys) distances in the case of the A centers. However in the B centers, the Cu-S(Cys) bonds elongate. Such behavior can be considered to be a result of the ligand-donation competition between the carbonyl and thiolate groups. The donation effect from a more distant methionine was found negligible in the A centers. In the B centers, the full optimization leads to a substantially different coordination arrangement (see ***Figure 4d***). The relaxed complex possesses a geometry halfway between square planar and tetrahedral arrangements, which has some impact on electronic properties as will be demonstrated later.

A lot of studies was devoted to investigation of protein constraints on the active centers of blue copper proteins. An earlier paper[94] suggested that there are no constraints. However, such a proposal was later revised[33,34,45]. The role of axial ligand has also been widely studied[5,33,46,47,49,95,96]. The section above provides some answers to the questions about constraints imposed by the protein backbone structure:

a) Neither oxidized nor reduced centers have optimum geometries. The extent of these forces can be estimated from the stabilization energies (cf. Section 3.2.1).

b) When no constraint is applied, the axial copper-ligand bond elongates/shortens depending on reduced/oxidized state of metal, regardless the type of 4th residue (Gln or Met).

c) Changes in coordination in reduced centers correspond to the fact that the Cu(I) complexes prefer geometry with a lower-coordination. Analogously, models of the fully relaxed oxidized Cu(II) centers tend to form four "equivalent" bonds as can be seen from unification of the Cu-N(His) bonds and shortening of the Cu-L distances of the 4th ligand.

3.1.3 Relaxed models in solvents

The studied redox centers are influenced by their environment. Such effects were examined at the QM/MM level[32,43,97]. Polarized continuum models were also used for this kind of complexes in ref.[43]. Given the model used in our calculations, the subtler differences within the individual families of (both Type A and B) proteins cannot be reproduced. However, the influence of solvent effects can be still estimated in the PCM regime through the screening of electrostatic interactions. These effects can be important for more accurate energy analyses.

In case of the oxidized Cu(II) centers, solvation effects exhibit a lower influence on the fully optimized geometries than in the reduced Cu(I) complexes. Screened electrostatic interaction of the thiolate Cu-S(Cys) bond results in a mild elongation with an increasing value of the dielectric constant. Since the donation effect is very distance-sensitive (it is linked to the overlap of Cu and S AOs), the cysteine donation weakens correspondingly. Simultaneously, shortening of the Cu-N(His) bonds occurs increasing the donation competition. Interestingly, the distance of the Cu-O(Gln) and Cu-S(Met) bonds also shorten. Such a behavior causes a dative competition between the Cys and all other (neutral) ligands. In the Gln case, the strengthening of the Cu-O(Gln) bond is in accord with the hard-soft-acid-base (HSAB) principle (oxygen is closer to the relatively hard Cu^{2+} cation than the sulfur atom[98]).

For the solvated Cu(I) centers, the Cu-S(Cys) distances elongate and similarly Cu-O(Gln) reflecting the reduced electrostatic enhancement in (implicit) solvent.

3.2 Energetics

Energy analyses and determination of electron properties in next the section were performed at the B3LYP/*6-311++G(2df,2pd)* level.

3.2.1 Stabilization energies

Stabilization ΔE^{Stab} and total coordination ΔE^{TCE} energies are presented in ***Table 3***. In the gas-phase calculations of the oxidized Cu(II) complexes, the stabilization energies of the B centers are about 6 kcal/mol higher than the ΔE^{Stab} energies of the A centers under the constrained optimization. For the reduced Cu(I) centers, the B centers are still more stable but less than 1 kcal/mol. When comparing the fully optimized structures, this difference remain similar in Cu(II) complexes but raises up to 9 kcal/mol in reduced states.

The difference [ΔE^{Stab}(full opt.) - ΔE^{Stab}(constrained opt.)] estimates a relaxation energy of ligands. This relaxation amounts up to 21 kcal/mol in case of the reduced B centers in the gas phase and up to 12 kcal/mol in water. Comparing changes in ΔE^{Stab} with ΔE^{TCE} when passing from the constrained to fully optimized structures for all three environments, it can be noticed that while stabilization (ΔE^{Stab}) always increases there are several cases where the ΔE^{TCE} energy for the fully optimized structures is even lower than the corresponding value for the constrained structures. This indicates that besides changes in the Cu-L coordinations, repulsion between the ligands is also minimized and some bonding interligand interactions can be formed. These interligand interactions can partially cause a decrease of particular

Cu-L bonding energy, which results in lower ΔE^{TCE} energy for fully optimized system.

Inclusion of the environment effects influences the stabilization energy as the screening decreases the electrostatic contribution to the bonding interaction between the Cu(I)/Cu(II) cation and ligands. Especially remarkable influence can be seen in the negatively charged model of cysteine. Therefore, the obtained ΔE^{Stab} values are pronouncedly lowered when compared to *in vacuo* calculations. The dielectric constant, proportionally lowers the stabilization energies. An interesting behavior was found when relaxation of the protein constraints (estimated as a difference of the ΔE^{Stab} energies of constrained and fully optimized structures) is considered. These values are drawn in ***Figure 5***. This Figure illustrates several trends: a) In both types of the centers, the reduced Cu(I) complexes are less stable under protein constraints than the oxidized complexes. b) The B centers exhibit a higher energy relaxation after full optimization. c) The relaxation energies are most pronounced in the gas phase calculations, where stabilization increases after full optimization up to 21 kcal/mol (cf. ***Table 3*** and ***Figure 5***).

3.2.2 Ligand bonding energies

Bonding energies ΔE^{BE} of all the ligands in the studied redox centers are compiled in ***Table 4***. Partitioning of the system into the ligand and the remaining part of the complex provides a useful insight into the strength of individual dative bonds. The Cu-S(Cys) coordination clearly dominates in all investigated complexes with the ΔE^{BE} energies *in vacuo* around 240 and 130 kcal/mol for the oxidized and reduced centers, respectively. Such high bonding energies are products of a dative coordination enhanced by a strong electrostatic interaction between the $Cu^{2+/+}$ cation and cysteine model $[S(CH_3)]^{1-}$. For the Cu(II) complexes, ΔE^{BE} of the Cu-N(His)

bonds are by an order of magnitude weaker, ranging from 28 kcal/mol (in constrained opt.) to 36 kcal/mol (in full opt.). Coordination of the acetyl group in the Cu-O(Gln) model was estimated to be about 11 kcal/mol for the restrained structure and about 20 kcal/mol for the fully optimized complex. The weakest bonding energies are visible for the thioether Cu-Met bonds, less than 13 kcal/mol. The coordination energy for the 4th residue reflects the shortening of these Cu-L bonds described in the geometry discussion above. It confirms the tendency for 4-coordination of the Cu(II) structures when no protein constraints are applied.

In the reduced centers, the Cu-L coordination bonds in protein imposed structures are noticeably weaker than in the Cu(II) case, mainly due to the reduction of electrostatic contributions. Actually, the ΔE^{BE} energies of the Cu-Met/Gln bonds exhibit negative values in our model. This can be explained by the fact that the ΔE^{BE} energies also contain an interligand repulsion, which can be stronger than weak Cu(I)-L attractive interaction. For the fully optimized complexes in vacuo (without protein constraints) no negative bonding energies were obtained since the repulsive ligand-ligand interactions were minimized. In the geometry discussion, it was proposed that the reduced centers tend to lower coordination numbers. A partial support for this statement can be seen in differences of the ΔE^{BE} values for the Cu-His1 and Cu-His2 bonds in the fully optimized structures. Here, one can notice that only two ΔE^{BE} energies of the Cu(I)-L bonds are higher than 6 kcal/mol in the gas-phase calculations, which can be interpreted that only two Cu(I)-L dative bonds are present in the reduced A centers. Such an argument is not convincing for the B centers in accord with higher stability of the 3-coordinated $[Cu(H_2S)(H_2O)(NH_3)_2]^+$ complexes.

3.2.3 Ionization potentials

In order to describe transition between the Cu(II) and Cu(I) oxidation states, vertical IP^{vert} and adiabatic IP^{adiab} ionization potentials were calculated according to the equation (2). The obtained values are listed in ***Table 5***. It can be noticed that the IP values decrease rapidly with an increasing relative permittivity. In the constrained optimizations, lower values of both vertical and adiabatic ***IP*** for the B centers can be seen regardless of the type of the environment. Optimized structures in all three environments display an inverted order of ***IP*** (***IP****(type A)* **<** ***IP****(type B))* for vertical transitions and for the adiabatic IP^{adiab} energies in vacuo and protein-like neighborhood. It can be noticed that structural relaxation leads to increase of IP values as one could expect according to larger stabilization of reduced complexes from ***Figure 5***. The more pronounced stabilization of reduced Type B centers (especially in gas phase and protein-like environment) is responsible for the inverted order of IP in these optimized (relaxed) complexes.

Experimentally obtained redox potentials E_0 for the studied proteins are presented in ***Table 6***. There are also recent calculations on the T-1 blue-copper-proteins reduction potential, which treats larger model and reproduce experimental results fairly accurately[99]. Although our calculations are not able to reveal E_0 values for individual proteins, it is at least partially possible to compare the relative differences between the A and B families. The difference of 0.14 eV obtained from experiment is in good agreement with the difference IP^{adiab}*(type A)* **-** IP^{adiab}*(type B)* (=0.19 eV) from the present work. There is relatively large variation of the redox potential of type A family (cf.Table 6) so one should take the comparison only as a qualitative insight.

3.3 Electron structure

Electron distributions of the redox centers of blue copper proteins were investigated in terms of the NPA partial charges, AIM and molecular orbital (MO) analysis, and spin densities together with the EPR spectra estimation.

3.3.1 Charge and spin density distribution

The electron spin densities in terms of partial atomic spin densities (ρ_s obtained by the NPA method) are summarized in ***Table 7***. Since there is a strong dative interaction between Cu^{2+} and cysteine model $[S(CH_3)]^-$, most of the spin density (80 - 90 %) is located on the Cu-S(Cys) bond as it can be observed in ***Figure 6***. The B centers exhibit a higher portion of spin density ρ_s on Cu and lower ρ_s on the sulfur atom of the cysteine model when compared to the A centers. It shows that in oxidized Type B centers, always lower donation occurs from cysteine sulfur than in Type A centers, leaving larger spin density on copper cation. This is linked with a stronger donation ability of the Gln residue (than Met). These analyses are in good accord with other computational works – similar picture was already obtained in study of De Kerpel et al.[100].

Partial atomic charges δ obtained by the NPA are compiled in ***Table 8*** for the copper cation and all the donating atoms. For both Cu(I) and Cu(II) complexes, atomic charges closely reflect the donation from the individual ligands. The partial charges give an insight on how much of electron density from the given atom is approximately involved in the (dative) bonding (cf. ***Tables 8***). It can be noticed that Type B centers exhibit in oxidized state lower donation from cysteine – in accord with spin densities (and AIM analysis) but (generally) slightly larger donation occurs in case of histidine ligands, which is also supported by larger electron densities in Cu-N critical points in AIM analysis. In the case of Cysteine (δ(S) = -0.74 e for isolated $[S(CH_3)]^-$ in vacuo), the partial charge is reduced (in absolute value) to -0.57 e in

structure of Cu(I) centers. It shows that polarization by the Cu cation causes shifting of the electron density towards the cation in all the ligands. Part of this electron density is then used for metal donation. In case of the Cu(II) complexes, the effect is even more pronounced resulting in the reduction of partial charge of sulfur atom as low as -0.13 e. This situation can be recognized as a transfer of almost the whole electron from Cys to Cu(II). The same description follows from the discussion of the electron spin densities (see above). In the Met residue, positive δ(S) values were found on the S atom in all cases. In the reduced centers, the sulfur partial charges do not change substantially compared to an isolated molecule, since the Cu(I)-S(Met) distances are very long. In the Cu(II) complexes, the partial charges in vacuo are lowered by about 0.04 e compared to the isolated $S(CH_3)_2$ molecule reflecting some shortening of the Cu-S(Met) bond in oxidized centers as well as their positive ΔE^{BE} bond energies. Results for the thioether ligand can be also compared with our previous study[79], where the $[Cu(H_2S)_n]^{2+/+}$ complexes (n = 1 – 4) with neutral hydrogen sulfide displayed δ(S) = -0.1 and -0.2 e for the Cu(II) and Cu(I) systems, respectively. These more negative values (in contrary to Met) are product of a much shorter coordination distances in these inorganic complexes.

Partial charge on the Cu atom was estimated to be about 0.96 and 0.69 e for the oxidized and reduced A centers in vacuo, respectively. For the Cu(II)/Cu(I) cations in the B centers, slightly higher values δ = 1.04/0.74 e were obtained. The difference can be explained by a weaker Cu-Cys donation in the B complexes, which represents the main contribution to the partial charge reduction of the copper cations. When solvation effects are considered, the Cu partial charge increases with a decreasing dative interaction of the ligands as a consequence of a bond elongation. It is a result of the more effective screening of electrostatic interactions, which enhances

the dative bonds especially in the case of negatively charged model of the Cysteine side chain.

3.3.2 Molecular orbitals analysis

In this part, only behavior of single occupied molecular orbitals (SOMO) in the oxidized centers will be discussed. The analysis revealed three types of SOMO, which are illustrated in ***Figure 7***. The first type (***7a***) represents a typical SOMO occurring in the A centers, which was also presented in some other works[45,47,49]. In this type, the $3p_{\pi}$ orbital of S(Cys) is combined with $3d_{x^2-y^2}$ AO of copper. The second type (***7b***) contains nonbonding admixture of S(Cys)$3p_z$ orbital perpendicular to the $3d_{x^2-y^2}$ AO of Cu. The fully optimized A centers and the protein structures of B centers possess this type of SOMO. In the third type of molecular orbital (***7c***), SOMO is dominantly composed of copper 3d AO's so that the lobes aim to all four Cu-ligand bonds.

3.3.3 EPR spectrum of oxidized centers

EPR spectra represent an important tool for investigation of the Cu(II) complexes, since the method is based on magnetic properties of the unpaired electrons. The key tensor property called the g-factor describes how a local magnetic field is induced by the external magnetic field. It approaches the value of 2.0023 for a single free electron. Similar values should be obtained for systems with delocalized unpaired electron. Otherwise, it can markedly rise. Main axes of the diagonalized g-tensor were determined for all the studied Cu(II) complexes (***Table 9***). Experimental values are listed as well. In case of the protein imposed structures, $g_{\parallel}$ and $g_{\perp}$ values *in vacuo* were estimated to be about 2.12 and 2.05 a.u., respectively. This anisotropic splitting of the g-factor is close to the experimental values (2.23 and 2.05) for the A centers of

the blue copper proteins[13,96]. Considering the solvent effects in the COSMO regime slightly improves the calculated $g_{\parallel}$ values. However, in order to obtain a better agreement with the experiment, the hybrid functional needs to be modified by fitting the ratio of the DFT exchange-correlation and the Hartree-Fock exchange terms as discussed e.g. in review[13]. On the other hand, the B3LYP functional successfully reproduces higher $g_{\parallel}$ values for the B centers, even in vacuo. The fully optimized A complex exhibits similar behavior as the protein structures from the database. In case of the B center, full optimization reveals a different trend, where $g_{\parallel}$ is very similar to $g_{\perp}$ = 2.08. Such behavior can be explained by pronounced geometry changes in the fully optimized B center with a more competitive Gln ligand as mentioned in the previous geometry discussion and demonstrated in ***Figure 4d***. In this way, extensive redistribution of unpaired electron occurs as it was already illustrated by plots of spin densities in ***Figure 6***.

For the solvated complexes, the distinction between $g_{\parallel}$ and $g_{\perp}$ increases with dielectric constant in the A centers as a reaction to the shortening of Cu-N bonds and concentrating electron density in N,N,S plane. On the contrary, the difference between both g components decreases in the B centers since a simultaneous increase of the Cu-S(Cys) and decrease of Cu-O(Gln) distances causes formation of a more symmetrical (isotropic) arrangement (cf. ***Table 1***).

4. Conclusions

Models of mononuclear centers of blue copper proteins were investigated in the present study. Two families of these proteins were examined: the Type A centers with methionine side chain as the fourth residue and the Type B centers with glutamine residue.

Selected structures were optimized at the B3LYP/*6-31+G(d)* level. Starting geometries of the complexes were taken from the PDB database (active centers from seven proteins – Type A: amicyanin, auracyanin, plastocyanin, rusticyanin; Type B: mavicyanin, stellacyanin, and umecyanin). Both reduced and oxidized states were investigated in the gas phase as well as in the implicit solvent regime (in COSMO approach) simulating water (ε=78) and protein-like environment (ε=4). First, in the constrained optimizations stage, the structural restrictions related to the presence of the protein matrix were partially taken into account. In the final step, all these constraints were released. Differences between both optimizations revealed that neither oxidized nor reduced structures of the copper centers stay in their optimum geometries. In comparison with the PDB structures, the axial Cu-L bond elongates/shortens depending on the reduced/oxidized state of the central metal, regardless the type of protein (A or B). In reduced centers, relaxation of coordination bonds corresponds to fact that the Cu(I) complexes prefer geometry with a lower coordination. Analogously, models of the fully relaxed oxidized Cu(II) centers tend to form four "equivalent" bonds.

Detailed insight into the properties of these Cu(I)/Cu(II) complexes is provided by energy analyses performed at the more accurate B3LYP/*6-31++G(2df,2pd)* level. According to differences in the stabilization energies with and without constraints, oxidized states of the both A and B centers are in average closer to the optimized geometries (as follows from the lower relaxation energies drawn in ***Figure 5***). Higher relaxation energy is released within the full optimization for the Type B centers.

Ionization potentials were used for characterization of the transitions between the Cu(II)/Cu(I) redox states. For constrained structures, ***IP***(type A) > ***IP***(type B)

trend was obtained regardless of the type of environment. In the case of fully optimized structures, the order is altered for vertical transitions in all three types of surroundings as well as for adiabatic transition *in vacuo* and protein like environment. Nevertheless, higher $\boldsymbol{IP^{adiab}}$ values were found for the A centers optimized within the COSMO approach for water. Such behavior reflects the ability of the solvent to influence the redox properties of the studied centers. Comparing relative difference between the constrained A and B proteins centers, the redox potential difference $\boldsymbol{\Delta E_0}$ = 0.20 eV was obtained, which is in accord with experimentally known data (of about 0.14 eV). But as already stated, this conclusion should be take with care due to large fluctuation in redox potential of the Type A proteines.

Charge and spin distributions were obtained by the NPA method. They revealed that most of the spin density (80-90%) is located on the Cu-S(Cys) bond, which corresponds to a strong (enhanced) dative interaction between the copper cation and cysteine. The B centers exhibit a higher portion of spin density on Cu as well as a higher partial charge localized on the Cu atom compared to the A centers. Such behavior reflects the stronger ability of the Gln ligand to donate electron density compared to the Met ligand.

For the Cu(II) complexes, characteristics of the EPR spectra (g-factors) were also estimated. Despite some differences occurred comparing calculated and experimental values of the $g_{\parallel}$ component, in general the anisotropy trend of the electron spin density was determined correctly. This can be also demonstrated on the maps of spin densities in ***Figure 6***. Interesting behavior was found for the fully optimized B center, for which a distinct EPR spectrum and character of SOMO orbital were found. This feature can be explained by a markedly different, (near-tetrahedral, i.e. more symmetrical) geometry of this complex.

.

Acknowledgement

This study was supported by MSM 0021620835 grants. We are grateful for the access to the excellent computational resources of the Charles University Meta-Centrum in Prague. A special thank must be given to the KFCHO department computer cluster administrator Dr. Šimánek.

References:

[1] J.A. Cowan: Inorganic Biochemistry: An Introduction. , VCH Publishers, New York, 1993.

[2] ProMiS: Prosthetic groups and Metal Ions in Protein Active Sites http://metallo.scripps.edu/PROMISE/CUMAIN.html (1998).

[3] E.I. Solomon: Spectroscopic Methods in Bioinorganic Chemistry: Blue to Green to Red Copper Sites. Inorg. Chem. 45 8012 (2006).

[4] X. Wang, S.M. Berry, Y. Xia, Y. Lu: The Role of Histidine Ligands in the Structure of Purple Cua Azurin. J. Am. Chem. Soc. 121 7449 (1999).

[5] A.E. Palmer, D.W. Randall, F. Xu, E.I. Solomon: Spectroscopic Studies and Electronic Structure Description of the High Potential Type 1 Copper Site in Fungal Laccase: Insight into Effect of the Axial Ligand. J Am. Chem. Soc. 121 7138 (1999).

[6] S. Santra, P. Zhang, W. Tan: Novel Interaction between Glutamate and the Cu2+ /DMABN/beta-CD Complex. J. Phys. Chem. A 104 12021 (2000).

[7] K. Shimizu, H. Maeshima, H. Yoshida, A. Satsuma, T. Hattori: Ligand field effect on the chemical shift in XANES spectra of Cu(II) compounds. Phys. Chem. Chem. Phys. 3 862 (2001).

[8] M.L. Barrett, I. Harvey, M. Sundararajan, R. Surendran, J.F. Hall, M.J. Ellis, M.A. Hough, R.W. Strange, I.H. Hillier, S.S. Hasnain: Atomic Resolution Crystal Structures, EXAFS, and Quantum Chemical Studies of Rusticyanin and Its Two Mutants Provide Insight into Its Unusual Properties. Biochem. 45 2927 (2006).

[9] P. Manikandan, B. Epel, D. Goldfarb: Structure of Copper(II)-Histidine Based Complexes in Frozen Aqueous Solutions As Determined from High-Field Pulsed Electron Nuclear Double Resonance. Inorg. Chem. 40 781 (2001).

[10] J.A. Sigman, B.C. Kwok, A. Gengenbach, Y. Lu: Design and Creation of Cu(II)-Binding Site in Cytochrome c Peroxidase that Mimics the Cub-heme Center in Terminal Oxidases. J Am. Chem. Soc. 121 8949 (1999).

[11] H.B. Gray, B.G. Malmstroem, R.J.P. Williams: Copper coordination in blue proteins. J. Biol. Inorg. Chem. 5 551 (2000).

[12] E.I. Solomon, M.J. Baldwin, M.D. Lowery: Electronic Structures of Active Sites in Copper Proteins: Contribution to Reactivity. Chem. Rev. 92 521 (1992).

[13] E.I. Solomon, R.K. Szilagyi, S.D. George, L. Basumallick: Electronic Structures of Metal Sites in Proteins and Models: Contribution to Function in Blue Copper Proteins. Chem. Rev. 104 419 (2004).

[14] L.M. Mirica, X. Ottenwaelder, T.D.P. Stack: Structure and Spectroscopy of Copper-Dioxygen Complexes. Chem. Rev. 104 1013 (2004).

[15] L.D. Book, D.C. Arnett, H. Hu, N.F. Scherer: Ultrafast Pump-Probe Studies of Excited-State Charge Transfer Dynamics in Blue Copper Proteins. J. Phys. Chem. A 102 4350 (1998).

[16] E. Fraga, M.A. Webb, G.R. Loppnow: Charge-Transfer Dynamics in Plastocyanin, a Blue Copper Protein, from Resonance Raman Intensities. J. Phys. Chem. 100 3278 (1996).

[17] A.W. Holland, R.G. Bergman: Heterocumulene Metathesis by Iridium Guanidinate and Ureylene Complexes: Catalysis Involving Reversible Insertion To Form Six-Membered Metallacycles. J. Am. Chem. Soc. 124 9010 (2002).

[18] P.L. Holland, W.B. Tolman: Three-Coordinate Cu(II) Complexes: Structural Models of Trigonal-Planar Type 1 Copper Protein Active Sites. J Am Chem. Soc. 121 7270 (1999).

[19] M.K. Taylor, D.E. Stevenson, L.E.A. Berlouis, A.R. Kennedy, J. Reglinski: Modelling the impact of geometric parameters on the redox potential of blue copper proteins. J. Innorg. Biochem. 100 250 (2005).

[20] D.F. Raffa, R. Gomez-Balderas, P. Brunelle, G.A. Rickard, A. Rauk: Ab initio model studies of copper binding to peptides containing a His-His sequence: relevance to the beta-amyloid peptide of Alzheimer's disease. J Biological Inorg. Chem. 10 887 (2005).

[21] J. Sabolovic, K.R. Liedl: Why are Cu(II) amino acid complexes not planar in their crystal structures? An ab initio and molecular mechanics study. Inorg. Chem. 38 2764 (1999).

[22] J. Sabolovic, C.S. Tautermann, T. Loerting, K.R. Liedl: Modeling anhydrous and aqua copper(II) amino acid complexes: A new molecular mechanics force field parametrization based on quantum chemical studies and experimental crystal data. Inorg. Chem. 42 2268 (2003).

[23] A. Katz, L. Shimoni-Livny, O. Navon, N. Navon, C. Bock, J. Glusker: Copper-binding motifs: Structural and theoretical aspects. HELVETICA CHIMICA ACTA (2003).

[24] L. Rulíšek: Theoretical studies of the interactions of transition metals with biomolecules. Chemicke Listy 96 132 (2002).

[25] L. Rulíšek, Z. Havlas: Theoretical Studies of Metal Ion Selectivity. 1. DFT Calculations of Interaction Energies of Amino Acid Side Chains with Selected Transition Metal Ions (Co2+, Ni2+, Cu2+, Zn2+, Cd2+, and Hg2+). J. Am. Chem. Soc. 122 10428 (2000).

[26] L. Rulíšek, Z. Havlas: Theoretical Studies of Metal Ion Selectivity. 3. A Theoretical Design of the Most Specific Metal-Binding Sites of Metalloproteins for Selected Transition Metal Ions (Co2+, Ni2+, Cu2+, Zn2+, Cd2+, and Hg2+). J. Phys. Chem. B 107 2376 (2003).

[27] J. Bertran, L. Rodrigues-Santiago, M. Sodupe: The Different Nature of Bonding in Cu+ -Glycine and Cu2+ -Glycine. J. Phys. Chem. B 103 2310 (1999).

[28] T. Shoeib, H.E. Aribi, K.W.M. Siu, A.C. Hopkinson: A Study of Silver (I) Ion-Organonitrile Complexes: Ion Structures, Binding Energies, and Substituent Effects. J. Phys. Chem. A 105 710 (2001).

[29] D. Caraiman, T. Shoeib, K. Siu, A. Hopkinson, D. Bohme: Investigations of the gas-phase reactivity of Cu+ and Ag+ glycine complexes towards CO, D2O and NH3. Int. J. Mass Spectrom. 228 629 (2003).

[30] M. Breza, S. Biskupic: On the reduced form of (imidazole-N-3)(N-salicylidene-alaninato-O,N,O ') copper(II). J Molecular Structure-Theochem 770 139 (2006).

[31] T. Shuku, K. Sugimori, A. Sugiyama, H. Nagao, T. Sakurai, K. Nishikawa: Molecular orbital analysis of active site of oxidized azurin: Dependency of electronic properties on molecular structure. Polyhedron 24 2665 (2005).

[32] M.H.M. Olsson, G.Y. Hong, A. Warshel: Frozen density functional free energy simulations of redox proteins: Computational studies of the reduction potential of plastocyanin and rusticyanin. J Am. Chem. Soc. 125 5025 (2003).

[33] M.H.M. Olsson, U. Ryde: The influence of axial ligands on the reduction potential of blue copper proteins. J. Biol. Inorg. Chem. 4 654 (1999).
[34] M.H.M. Olsson, U. Ryde, B.O. Roos, K. Pierloot: On the relative stability of tetragonal and trigonal Cu(II) complexes with relevance to the blue copper proteins. J. Biol. Inorg. Chem. 3 109 (1998).
[35] S. Corni, F. De Rienzo, R. Di Felice, E. Molinari: Role of the electronic properties of azurin active site in the electron-transfer process. International J Quantum Chem. 102 328 (2005).
[36] A. Warshel: Computer Modeling of Chemical Reactions in Enzymes and Solutions, John Wiley & Sons, Ltd., New York, 1991.
[37] R. Prabhakar, P.E.M. Siegbahn: Theoretical study of the mechanism for the oxidative half-reaction of copper amine oxidase (CAO). J Physical Chem. B 107 3944 (2003).
[38] K. Yoshizawa, Y. Shiota: Conversion of methane to methanol at the mononuclear and dinuclear copper sites of particulate methane monooxygenase (pMMO): A DFT and QM/MM study. J Am. Chem. Soc. 128 9873 (2006).
[39] M. van den Bosch, M. Swart, J.G. Snijders, H.J.C. Berendsen, A.E. Mark, C. Oostenbrink, W.F. van Gunsteren, G.W. Canters: Calculation of the redox potential of the protein azurin and some mutants. Chembiochem 6 738 (2005).
[40] Siegbahn, in I. Prigogine, S.A. Rice (Eds.), Advances in Chem. Physics, Volume XCIII. John Wilet & Sons, Ltd., 1996, p. 333.
[41] K.W. Penfield, A.A. Gewirth, E.I. Solomon: J. Am. Chem. Soc. 107 4519 (1985).
[42] A.A. Gewirth, E.I. Solomon: J. Am. Chem. Soc. 110 3811 (1988).
[43] S. Sinnecker, F. Neese: QM/MM calculations with DFT for taking into account protein effects on the EPR and optical spectra of metalloproteins. Plastocyanin as a case study. J Computational Chem. 27 1463 (2006).
[44] L.B. LaCroix, S.E. Shadle, Y.N. Wang, e. al: Electronic structure of the perturbed blue copper site in nitrite reductase: Spectroscopic properties, bonding, and implications for the entatic/rack state. J. Am. Chem. Soc. 118 7755 (1996).
[45] K. Pierloot, J.O.A. De Kerpel, U. Ryde, B.O. Roos: J. Am. Chem. Soc. 119 218 (1997).
[46] D.W. Randall, S.D. George, B. Hedman, K.O. Hodgson, K. Fujisawa, E.I. Solomon: Spectroscopic and Electronic Structural Studies of Blue Copper Model Complexes. 1. Perturbation of the Thiolate-Cu Bond. J. Am. Chem. Soc. 122 11620 (2000).
[47] L.B. LaCroix, D.W. Randall, A.M. Nersissian, e. al: Spectroscopic and geometric variations in perturbed blue copper centers: Electronic structures of stellacyanin and cucumber basic protein J. Am. Chem. Soc. 120 (1998).
[48] D.W. Randall, D.R. Gamelin, L.B. LaCroix, E.I. Solomon: Electronic structure contributions to electron transfer in blue Cu and Cua. J. Biol. Inorg. Chem. 5 15 (2000).
[49] J.A. Guckert, M.D. Lowery, E.I. Solomon: ELECTRONIC-STRUCTURE OF THE REDUCED BLUE COPPER ACTIVE-SITE - CONTRIBUTIONS TO REDUCTION POTENTIALS AND GEOMETRY. J. Am. Chem. Soc. 117 2817 (1995).
[50] K.J. de Almeida, R. Z., H.W. Hugosson, A.C. Ferreira, H. Agren: Modeling of EPR parameters of copper(II) aqua complexes Chem. Phys. 332 176 (2007).

[51] C. Remenyi, R. Reviakine, M. Kaupp: Density Functional Study of EPR Parameters and Spin-Density Distribution of Azurin and Other Blue Copper Proteins. J. Phys. Chem. B 111 8290 (2007).
[52] K. Ando: Excited State Potentials and Ligand Force Field of a Blue Copper Protein Plastocyanin
J. Phys. Chem. B 108 3940 (2004).
[53] K. Ando: Ligand-to-Metal Charge-Transfer Dynamics in a Blue Copper Protein Plastocyanin: A
Molecular Dynamics Study. J. Phys. Chem. B 112 250 (2008).
[54] P. Comba, R. Remenyi: A New Molecular Mechanics Force Field for the Oxidized Form of Blue Copper Proteins. J. Comput. Chem. 23 697 (2002).
[55] P. Comba, A. Lledo´s, F. Maseras, R. Remenyi: Hybrid quantum mechanics/molecular mechanics studies of the active site of the blue copper proteins amicyanin and rusticyanin. Inorg. Chim. Acta 324 21 (2001).
[56] P. Frank, M. Benfatto, R.K. Szilagyi, P. D'Angelo, S. Della Longa, K.O. Hodgson: The solution structure of [Cu(aq)](2+) and its implications for rack-induced bonding in blue copper protein active. Inorg. Chem. 44 1922 (2005).
[57] M. Konopka, R. Rousseau, I. Stich, D. Marx: Detaching thiolates from copper and gold clusters: Which bonds to break? J. Am. Chem. Soc. 126 12103 (2004).
[58] H. Tachikawa: Ab initio MRSDCI calculations of the g-tensor components of [Cu(H2O)6]2+ complexes. Chem. Phys.Lett. 260 582 (1996).
[59] I.P. Hamilton: Complexes of cationic coinage metal clusters M-n(+) (M = Cu, Ag, Au; n=1-4) and H2S: a theoretical study. Chem. Phys. Lett. 390 517 (2004).
[60] G.W. Marini, K.R. Liedl, B.M. Rode: Investigation of Cu2+ Hydration and the Jahn-Teller Effect in Solution by QM/MM MC Simulations. J. Phys. Chem. A 103 11387 (1999).
[61] C. Schwenk, B. Rode: Cu-II in liquid ammonia: An approach by hybrid quantum-mechanical/molecular-mechanical molecular dynamics simulation. CHEMPHYSCHEM 5 (3) (2004).
[62] C. Schwenk, B. Rode: Influence of heteroligands on structural and dynamical properties of hydrated Cu2+: QM/MM MD simulations. PHYSICAL CHEMISTRY CHEMICAL PHYSICS 5 (16) (2003).
[63] H. Pranowo: Monte Carlo simulation of CuCl2 in 18.6% aqueous ammonia solution. CHEMICAL PHYSICS 291 (2) (2003).
[64] H.D. Pranowo, B.M. Rode: Solvation of Cu2+ in Liquid Ammonia: Monte Carlo Simulation Including Three-Body Corrections. J. Phys. Chem. A 103 4298 (1999).
[65] H.D. Pranowo, A.H.B. Setiajin, B.M. Rode: Cu+ in Liquid Ammonia and in Water: Intermolecular Potential Function and Monte Carlo Simulation. J. Phys. Chem. A 103 11115 (1999).
[66] D. Feller, E.D. Glendening, W.A. de Jong: Structures and binding enthalpies of M + (H2O)n clusters, M = Cu, Ag, Au. J. Chem. Phys. 110 1475 (1999).
[67] D. Schroeder, H. Schwartz, J. Wu, C. Wesdemiotis: Long-lived dications of Cu(H2O)2+ and Cu(NH3)2+ do exist! Chem. Phys. Lett. 343 258 (2001).
[68] H.D. Pranowo, B.M. Rode: Prefential Cu2+ solvation in aqueous ammonia solution of various concetrations. Chem. Phys 263 1 (2001).

[69] F. Haeffner, T. Brinck, M. Haeberlein, C. Moberg: Force field parametrization of copper(I)-olefin systems from density functional calculations. Chem. Phys. Letters 397 39 (1997).
[70] N.M.D.S. Cordeiro, J.A.N.F. Gomes: Ab Initio Copper-Water Interaction Potential for the Simulation of Aqueous Solutions. J. Comput. Chem. 14 629 (1993).
[71] V. Subramanian, C. Shankaranarayanan, B.U. Nair, M. Kanthimathi, R. Manickkavachagam, T. Ramasami: Development of force field for some copper(II) Schiff-base complexes. Chem. Phys. Lett. 274 275 (1997).
[72] N. Gresh, C. Policar, C. Giessner-Prettre: Modeling Copper(I) Complexes: SIBFA Molecular Mechanics versus ab Inition Energetics and Geometrical Arrangements. J. Phys. Chem. 106 5660 (2002).
[73] M. Ledecq, F. Lebon, F. Durant, C. Giessner-Prettre, A. Marquez, N. Gresh: Modeling of copper(II) complexes with the SIBFA polarizable molecular mechanics procedure. Application to a new class of HIV-1 protease inhibitors. JOURNAL PHYSICAL CHEMISTRY B 107 (38) (2003).
[74] P. Schwerdtfeger, R.P. Krawczyk, A. Hammerl, R. Brown: A comparison of structure and stability between the group 11 halide tetramers M4X4 (M= Cu, Ag, or Au; X = F, Cl, Br, or I) and the group 11 chloride and bromide phosphanes (XMPH3)(4). Inorg. Chem. 43 6707 (2004).
[75] A. Berces, T. Nukada, P. Margl, T. Ziegler: Solvation of Cu2+ in Water and Ammonia. Insight from Static and Dynamical Density Functional Theory. J. Phys. Chem. A 103 9693 (1999).
[76] F. Neese: Sum-over-states based multireference ab initio calculation of EPR spin Hamiltonian parameters for transition metal complexes. A case study. Magn. Res. Chem. 42 S187 (2004).
[77] J.V. Burda, M. Pavelka, M. Šimánek: Theoretical model of copper Cu(I)/Cu(II) hydration. DFT and ab initio quantum chemical study. J. Molec. Struct. THEOCHEM 683 183 (2004).
[78] M. Pavelka, J.V. Burda: Theoretical model of copper Cu(I)/Cu(II) mixed aqua-amine complexes. DFT and ab initio quantum chemical study. Chem. Phys. 312 193 (2005).
[79] M. Pavelka, M. Šimánek, J. Šponer, J.V. Burda: Copper Cation Interactions with Biologically Essential Types of Ligands: A Computational DFT Study. J. Phys. Chem. A 110 4795 (2006).
[80] H.M. Berman, J. Westbrook, Z. Feng, G. Gilliland, T.N. Bhat, H. Weissig, I.N. Shindyalov, P.E. Bourne: The Protein Data Bank. Nucleic Acids Research 28 235 (2000).
[81] M.M. Hurley, L.F. Pacios, P.A. Christiansen, R.B. Ross, W.C. Ermler: Ab Initio Relativistic Effective Potentials with Spin-Orbit Operators. II. K through Kr. J. Chem. Phys. 84 6840 (1986).
[82] A. Klamt: J. Phys. Chem. 99 2224 (1995).
[83] A. Klamt, G. Schuurmann: Cosmo - a New Approach to Dielectric Screening in Solvents with Explicit Expressions for the Screening Energy and Its Gradient. J Chem. Soc.-Perkin Transactions 2 799 (1993).
[84] S.F. Boys, F. Bernardi: The Calculation of Small Molecular Interactions by the Differences of Separate Total Energies. Some Procedures with Reduced Errors. Mol. Phys. 19 553 (1970).

[85] T. Zimmermann, J.V. Burda: Cisplatin Interaction with Cysteine and Methionine in Aqueous Solution: Computational DFT/PCM Study. J. Comput. Chem. (2008).
[86] J. Šponer, M. Sabat, J.V. Burda, A.M. Doody, J. Leszczynski, P. Hobza: Stabilization of the Purine.Purine.Pyrimidine DNA Base Triplets by Divalent Metal Cations. J. Biomol. Structure Dynamics 16 139 (1998).
[87] A.E. Reed, R.B. Weinstock, F. Weinhold: Natural population analysis. J. Chem. Phys. 83 735 (1985).
[88] M.J. Frisch, J.A. Pople, J.S. Binkley: Self-Consistent Molecular Orbital Methods 25. Supplementary Functions for Gaussian Basis Sets. J. Chem. Phys. 80 3265 (1984).
[89] F. Weinhold, NBO 5.0 Program University of Wisconsin, Madison, Wisconsin 53706, Wisconsin, 2001.
[90] R.F.W. Bader: Atoms in Molecules: A Quantum Theory, Oxford Univ. Press, Oxford, 1990.
[91] G. Schaftenaar, J.H. Noordik: Molden: a pre- and post-processing program for molecular and electronic structures. J. Comput.-Aided Mol. Design 14 123 (2000).
[92] P.F. Flükiger: Development of the molecular graphics package MOLEKEL and its application to selected problems in organic and organometallic chemistry, Thèse No 2561, Département de chimie physique, Université de Genève, 1992. http://www.cscs.ch/molekel/.
[93] S. Portmann, H.P. Lüthi: MOLEKEL: An Interactive Molecular Graphics Tool. Chimia 54 766 (2000).
[94] U. Ryde, M.H.M. Olsson, K. Pierloot, B.O. Roos: J. Mol. Biol. 261 586 (1996).
[95] D.W. Randall, S.D. George, P.L. Holland, B. Hedman, K.O. Hodgson, W.B. Tolman, E.I. Solomon: Spectroscopic and Electronic Structural Studies of Blue Copper Model Complexes. 2. Comparison of Three- and Four-Coordinate Cu(II)-Thiolate Complexes and Fungal Laccase. J. Am. Chem. Soc. 122 11632 (2000).
[96] E.I. Solomon, K.W. Penfield, A.A. Gewirth, e. al: Electronic structure of the oxidized and reduced blue copper sites: Contributions to the electron transfer pathway, reduction potential, and geometry. Inorg. Chim. Acta 243 67 (1996).
[97] S.N. Datta, J. Sudhamsu, A. Pandey: Theoretical determination of the standard reduction potential of plastocyanin in vitro. J. Phys. Chem. B 108 8007 (2004).
[98] R.G. Parr, R.G. Pearson: HSAB. J. Am. Chem. Soc. 105 7512 (1983).
[99] H. Li, S.P. Webb, J. Ivanic, J.H. Jensen: Determinants of the Relative Reduction Potentials of Type-1 Copper Sites in Proteins. J. Am. Chem. Soc. 126 8010 (2004).
[100] J.A.O. De Kerpel, K. Pierloot, U. Ryde, B.O. Roos: Theoretical Study of the Structural and Spectroscopic Properties of Stellacyanin. J. Phys. Chem. B 102 4638 (1998).

Table 1. Coordination distances for oxidized Cu(II) and reduced Cu(I) complexes of the A and B centers of blue copper proteins (in Å). Bond lengths for structures obtained in both constrained and full optimization are presented. The optimizations were performed in vacuo, protein-like, and water environment. **Bold** indicates the averaged PDB distances, which are not changed in the optimization phase I.

		Oxidized Type A center			Oxidized Type B center		
		in vacuo	protein-like	water	in vacuo	protein-like	water
Cu-S(Cys)	Constr. opt		**2.204**			**2.196**	
	Full opt.	2.184	2.204	2.230	2.252	2.262	2.270
Cu-N(His)	Constr. opt		**1.948**			**1.947**	
	Full opt.	2.036	2.021	2.019	2.042	2.027	2.022
Cu-N(His)	Constr. opt		**2.043**			**2.035**	
	Full opt.	2.054	2.034	2.026	2.059	2.039	2.032
Cu-S(Met)/	Constr. opt		**2.889**			**2.190**	
Cu-O(Gln)	Full opt.	2.567	2.535	2.494	2.043	2.039	2.034
		Reduced Type A center			Reduced Type B center		
		in vacuo	protein-like	water	in vacuo	protein-like	water
Cu-S(Cys)	Constr. opt		**2.190**			**2.198**	
	Full opt.	2.190	2.211	2.218	2.199	2.218	2.226
Cu-N(His)	Constr. opt		**1.969**			**2.014**	
	Full opt.	1.995	2.063	2.106	2.031	2.032	2.030
Cu-N(His)	Constr. opt		**2.098**			**2.069**	
	Full opt.	2.225	2.066	2.027	2.131	2.090	2.082
Cu-S(Met)/	Constr. opt		**2.852**			**2.284**	
Cu-O(Gln)	Full opt.	4.430	4.662	4.974	3.728	3.854	3.845

Table 2. Average Cu-X (S, O, N) bond lengths (in Å) for small $[Cu(H_2S)_m(H_2O)_n(NH_3)_k]^{2+/+}$ models[79] and corresponding values obtained from CSD database by Katz et al.[23].

Cu(II)	Small models			CSD		
	4-coord.	5-coord.	6-coord.	4-coord.	5-coord.	6-coord.
Cu-N	2.03	2.09	2.28	1.98	2.03	2.34
Cu-O	2.01	2.06	2.13	1.93	2.07	2.36
Cu-S	2.40	2.49	2.41	2.28	2.43	2.72
Cu(I)	Small models			CSD		
	2-coord.	3-coord.	4-coord.	2-coord.	3-coord.	4-coord.
Cu-N	1.91	2.02	2.12	1.90	1.98	2.04
Cu-O	1.88	2.04	2.21	1.84	2.14	2.05
Cu-S	2.19	2.29	2.35	2.17	2.26	2.33

Table 3. ΔE^{stab} stabilization and ΔE^{TCE} sterically corrected stabilization energies (in kcal/mol) for oxidized Cu(II) and reduced Cu(I) complexes of the A and B centers of blue copper proteins. Energies are presented for structures obtained by all optimization schemes with and without environment effects.

		Oxidized Type A center			Oxidized Type B center		
		in vacuo	protein-like	water	in vacuo	protein-like	water
ΔE^{stab}	Constr. opt	589.9	330.3	256.7	595.4	332.3	258.2
	Full opt.	596.4	336.3	263.3	602.0	339.0	265.1
ΔE^{TCE}	Constr. opt	616.9	372.6	298.7	631.2	383.9	308.1
	Full opt.	619.7	380.4	309.8	623.9	384.5	308.4
		Reduced Type A center			Reduced Type B center		
		in vacuo	protein-like	water	in vacuo	protein-like	water
ΔE^{stab}	Constr. opt	229.4	125.1	96.9	229.4	123.9	95.0
	Full opt.	242.0	132.9	104.6	250.9	138.4	106.9
ΔE^{TCE}	Constr. opt	254.6	165.9	137.5	258.3	169.3	140.6
	Full opt.	254.9	166.2	134.9	254.3	164.9	131.2

Table 4. ΔE^{BE} bond energies (in kcal/mol) for oxidized Cu(II) and reduced Cu(I) complexes of the A and B centers in various environments.

		Oxidized type A center			Oxidized type B center		
		in vacuo	protein like	water	in vacuo	protein like	water
Cu-S(Cys)	Constr. opt	242.6	105.4	65.2	238.7	108.7	75.5
	Full opt.	240.1	100.2	56.7	234.2	96.3	70.2
Cu-N(His)	Constr. opt	31.5	26.0	24.4	28.9	22.5	21.4
	Full opt.	33.6	25.5	19.7	33.3	27.0	30.3
Cu-N(His)	Constr. opt	35.7	24.3	22.6	28.9	22.2	21.1
	Full opt.	28.4	20.8	22.2	28.4	21.0	23.0
Cu-S(Met)/	Constr. opt	4.6	0.0	-1.0	10.9	2.4	0.6
Cu-O(Gln)	Full opt.	13.2	8.9	10.1	20.3	23.9	25.8
		Reduced type A center			Reduced type B center		
		in vacuo	protein like	water	in vacuo	protein like	water
Cu-S(Cys)	Constr. opt	109.2	41.0	23.2	106.8	39.6	22.4
	Full opt.	130.6	54.7	42.8	131.7	57.3	43.0
Cu-N(His)	Constr. opt	8.2	6.6	7.2	5.7	3.8	4.7
	Full opt.	22.5	12.3	24.3	20.6	16.7	21.1
Cu-N(His)	Constr. opt	3.7	1.9	2.5	3.2	0.2	0.9
	Full opt.	5.9	10.9	5.9	10.0	8.7	11.5
Cu-S(Met)/	Constr. opt	-2.2	-4.9	-5.4	-1.5	-6.8	-7.4
Cu-O(Gln)	Full opt.	3.7	-4.1	-2.7	15.8	3.1	-4.7

Table 5. Vertical and adiabatic ionization potentials (in eV) representing transition from reduced to oxidized state. Values are presented for both the A and B centers obtained in vacuo as well as in protein-like and water environment.

		Vertical ionization			Adiabatic ionization		
	Center	in vacuo	protein-like	water	in vacuo	protein-like	water
Constr. opt.	A	5.03	4.29	4.15	4.97	4.23	4.08
	B	4.85	4.13	4.00	4.73	4.04	3.93
Full opt.	A	5.92	5.08	4.92	5.22	4.30	4.33
	B	6.03	5.27	5.06	5.36	4.39	4.13

Table 6. Redox potentials (in mV) for selected blue copper proteins[12].

protein		redox potential
Type A	amicyanin	261
	auracyanin	240
	plastocyanin	370
	rusticyanin	680
	averaged	**388**
Type B	mavicyanin	285
	stellacyanin	184
	umecyanin	283
	averaged	**251**

Table 7. Spin electron density (in e) localized on copper, cysteine model, and the rest of complex obtained by the NPA method for oxidized Cu(II) complexes of the A and B centers.

			Spin density		
			Cu	S(Cys)	N,N,S/O
Type A center	in vacuo	Constr. opt	0.34	0.56	0.09
		Full opt.	0.38	0.50	0.12
	protein-like	Constr. opt	0.40	0.48	0.12
		Full opt.	0.44	0.39	0.18
	water	Constr. opt	0.43	0.44	0.13
		Full opt.	0.48	0.32	0.20
Type B center	in vacuo	Constr. opt	0.39	0.51	0.10
		Full opt.	0.53	0.30	0.17
	protein-like	Constr. opt	0.47	0.41	0.13
		Full opt.	0.56	0.25	0.19
	water	Constr. opt	0.50	0.36	0.14
		Full opt.	0.57	0.23	0.19

Table 8. Partial atomic charges (in e) on copper and coordinated atoms S(Cys), N(His), S(Met), and O(Gln) obtained by the NPA method.

		Oxidized Type A center			Oxidized Type B center		
		in vacuo	protein-like	water	in vacuo	protein-like	water
Cu	Constr. opt	0.961	1.016	1.043	1.042	1.110	1.140
	Full opt.	0.976	1.032	1.059	1.166	1.197	1.208
S(Cys)	Constr. opt	-0.130	-0.225	-0.272	-0.174	-0.292	-0.346
	Full opt.	-0.209	-0.312	-0.387	-0.350	-0.424	-0.457
N(His)	Constr. opt	-0.634	-0.650	-0.655	-0.625	-0.651	-0.656
	Full opt.	-0.639	-0.661	-0.646	-0.645	-0.639	-0.658
N(His)	Constr. opt	-0.652	-0.657	-0.661	-0.644	-0.643	-0.649
	Full opt.	-0.632	-0.642	-0.665	-0.628	-0.655	-0.643
S(Met)/ O(Gln)	Constr. opt	0.190	0.184	0.183	-0.738	-0.755	-0.770
	Full opt.	0.225	0.237	0.258	-0.762	-0.770	-0.775
		Reduced Type A center			Reduced Type B center		
		in vacuo	protein-like	water	in vacuo	protein-like	water
Cu	Constr. opt	0.697	0.712	0.715	0.737	0.750	0.752
	Full opt.	0.648	0.687	0.686	0.675	0.693	0.698
S(Cys)	Constr. opt	-0.573	-0.647	-0.678	-0.570	-0.652	-0.684
	Full opt.	-0.561	-0.633	-0.659	-0.546	-0.624	-0.654
N(His)	Constr. opt	-0.594	-0.613	-0.626	-0.590	-0.623	-0.635
	Full opt.	-0.598	-0.622	-0.628	-0.586	-0.623	-0.635
N(His)	Constr. opt	-0.604	-0.630	-0.643	-0.603	-0.616	-0.631
	Full opt.	-0.582	-0.622	-0.637	-0.603	-0.614	-0.651
S(Met)/ O(Gln)	Constr. opt	0.223	0.205	0.197	-0.676	-0.708	-0.735
	Full opt.	0.194	0.185	0.184	-0.718	-0.732	-0.742

Table 9. EPR g-factors for all studied Cu(II) centers (in a.u.). Experimental values taken from ref.[12].

		Exp.	in vacuo		protein-like		water	
			Constr.	Full opt.	Constr.	Full opt.	Constr.	Full opt.
Type A	$g_{\parallel}$	2.226	2.115	2.131	2.131	2.137	2.138	2.143
	$g_{\perp}$	2.045	2.052	2.056	2.058	2.061	2.061	2.065
Type B	$g_{\parallel}$	2.297	2.123	2.085	2.140	2.090	2.147	2.120
	$g_{\perp}$	2.051	2.058	2.079	2.066	2.082	2.070	2.073

Captions to Figures:

Figure 1: PDB structure of plastocyanin (1KDI).

Figure 2: Models of ***a)*** Type A and ***b)*** Type B centers of blue copper proteins. Family of Type A centers includes following peptides: amicyanin, auracyanin, plastocyanin, and rusticyanin. In case of the Type B centers, following proteins were considered: mavicyanin, stellacyanin, and umecyanin.

Figure 3: Example of 4-coordinated $[Cu(H_2S)_2(NH_3)_2]^{2+}$ complex, where transition from Cu(II) to Cu(I) state goes along with pronounced structural change from square-planar to tetrahedral ligand arrangement. When the system is even more relaxed, it evolves to 2-coordinated structure.

Figure 4: Structures of reduced ***a)*** Type A and ***b)*** Type B centers after the full optimization in vacuo. Optimized structure of oxidized centers of ***c)*** Type A and ***d)*** Type B are presented too.

Figure 5: The relaxation energies (in kcal/mol), determined as relative differences of ΔE^{Stab} energies of constrained and fully optimized structures for:

_■_ oxidized Type A centers,
--♦-- oxidized Type B centers,
-.-▲-.- reduced Type A centers, and
…▼… reduced Type B centers.

Figure 6: Plots of spin isodensities (ρ_s = 0.01 e/Å^3) for selected Cu(II) complexes. Oxidized ***a)*** Type A (plastocyanin) and ***b)*** Type B (umecyanin) centers with imposed protein geometry (constrained opt.) and ***c)*** Type A and ***d)*** Type B centers after full optimization are considered.

Figure 7: Three different schemes of SOMO with examples. The ***a)*** scheme occurs in Type A centers (opt. phase I), ***b)*** scheme is in Type A (full opt.) and Type B (opt. phase I) complexes, and ***c)*** can be found in fully optimized Type B center.

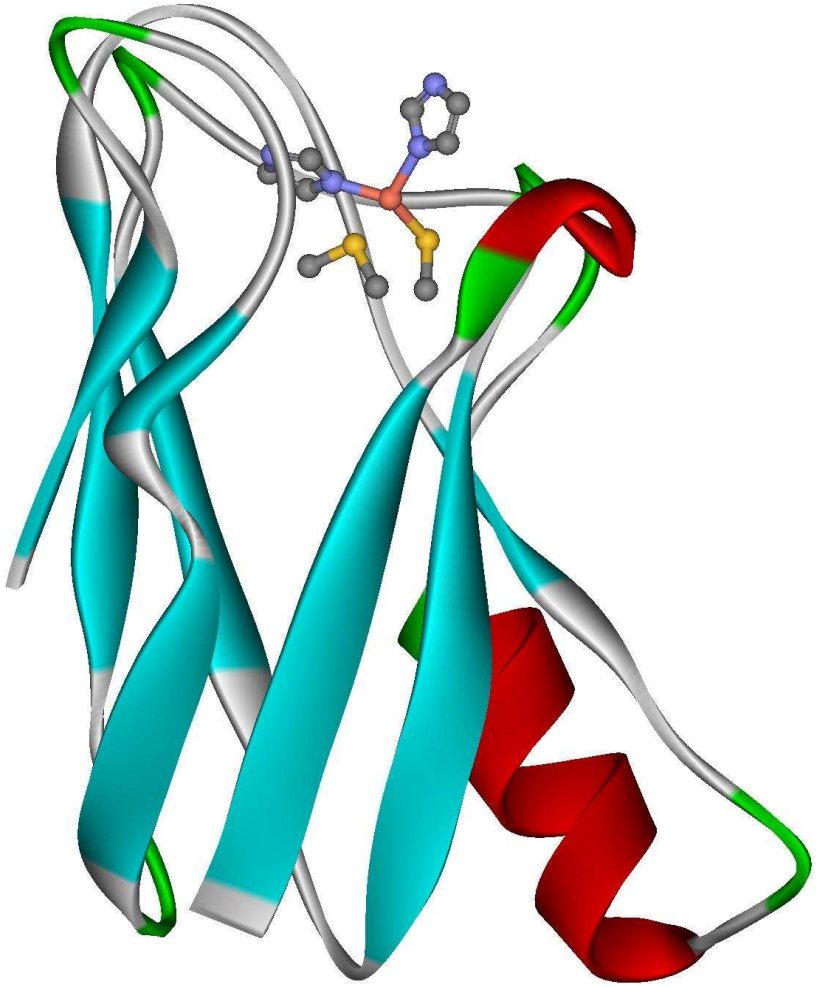

Figure 1:

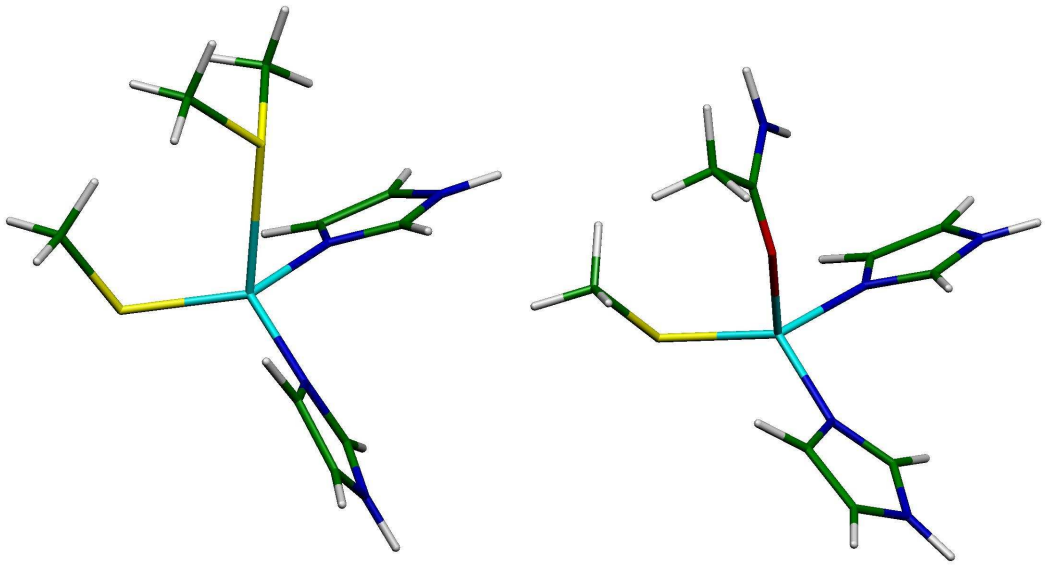

Figure 2

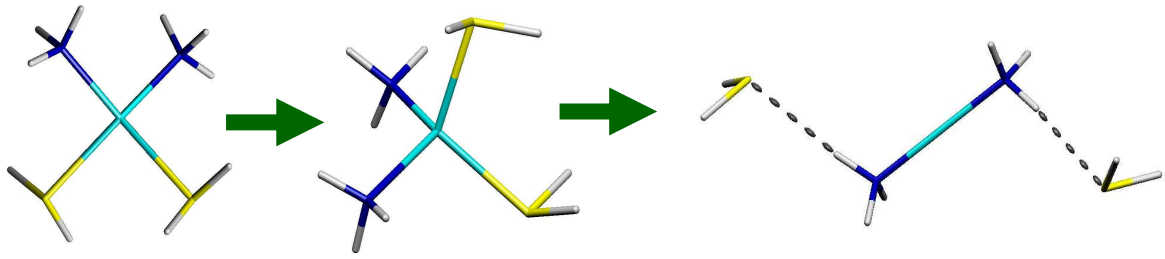

Figure 3

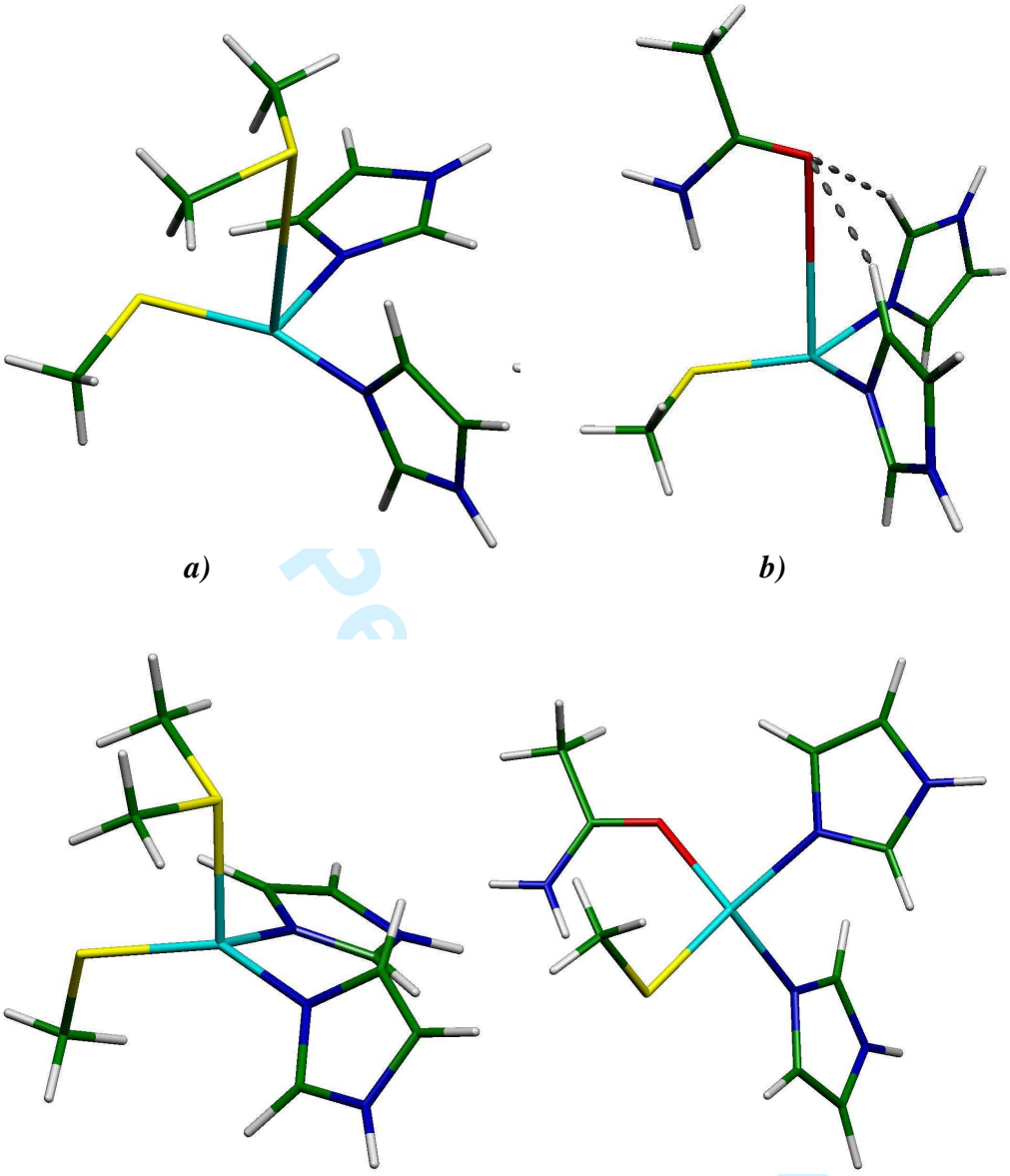

Figure 4

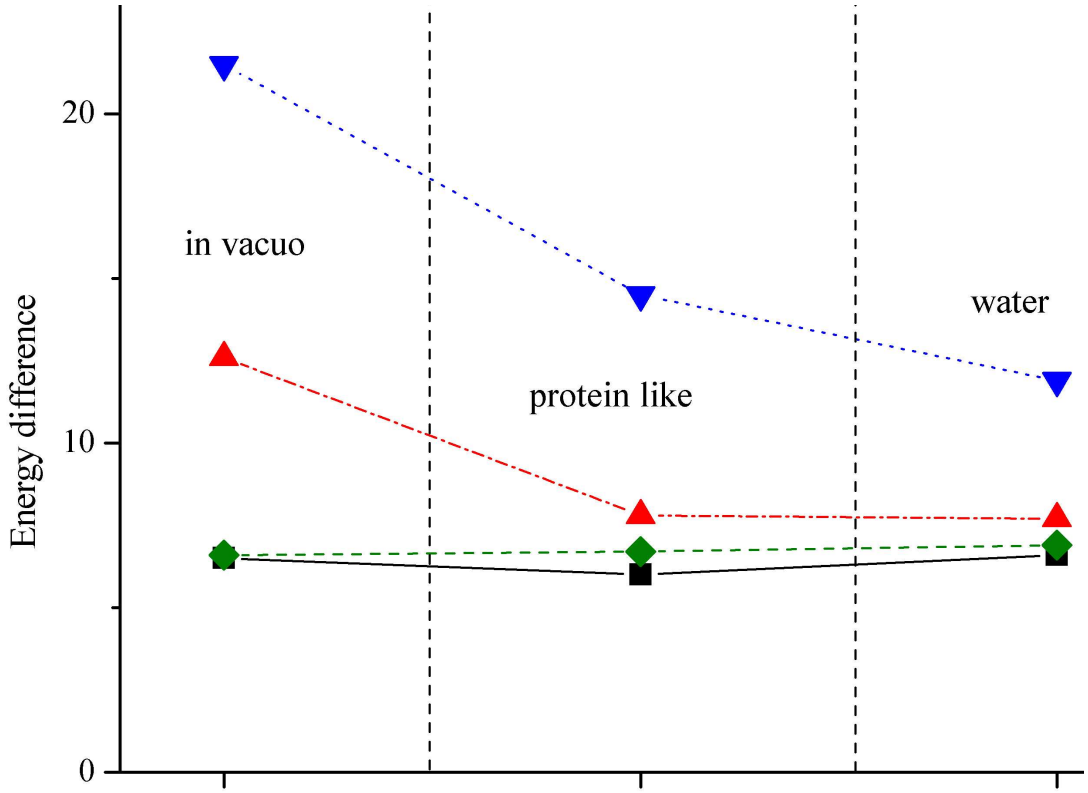

Figure 5

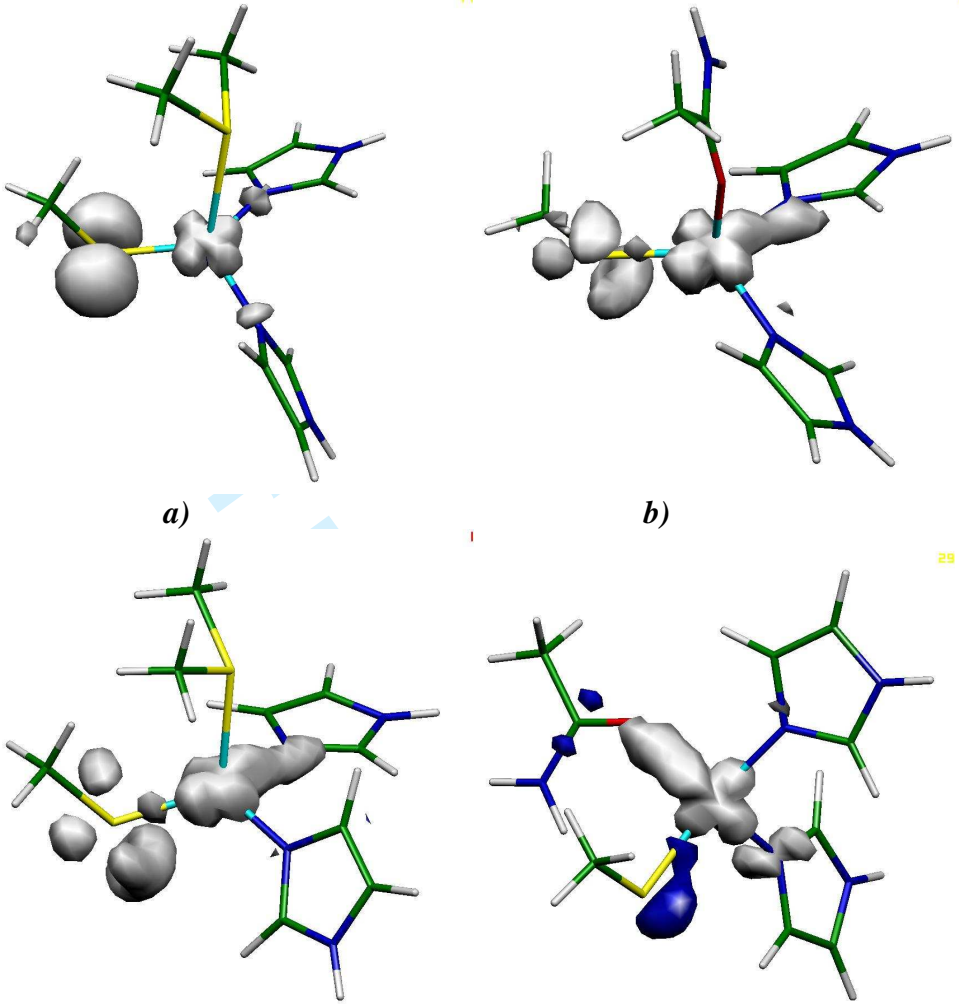

a) *b)*

c) *d)*

Figure 6

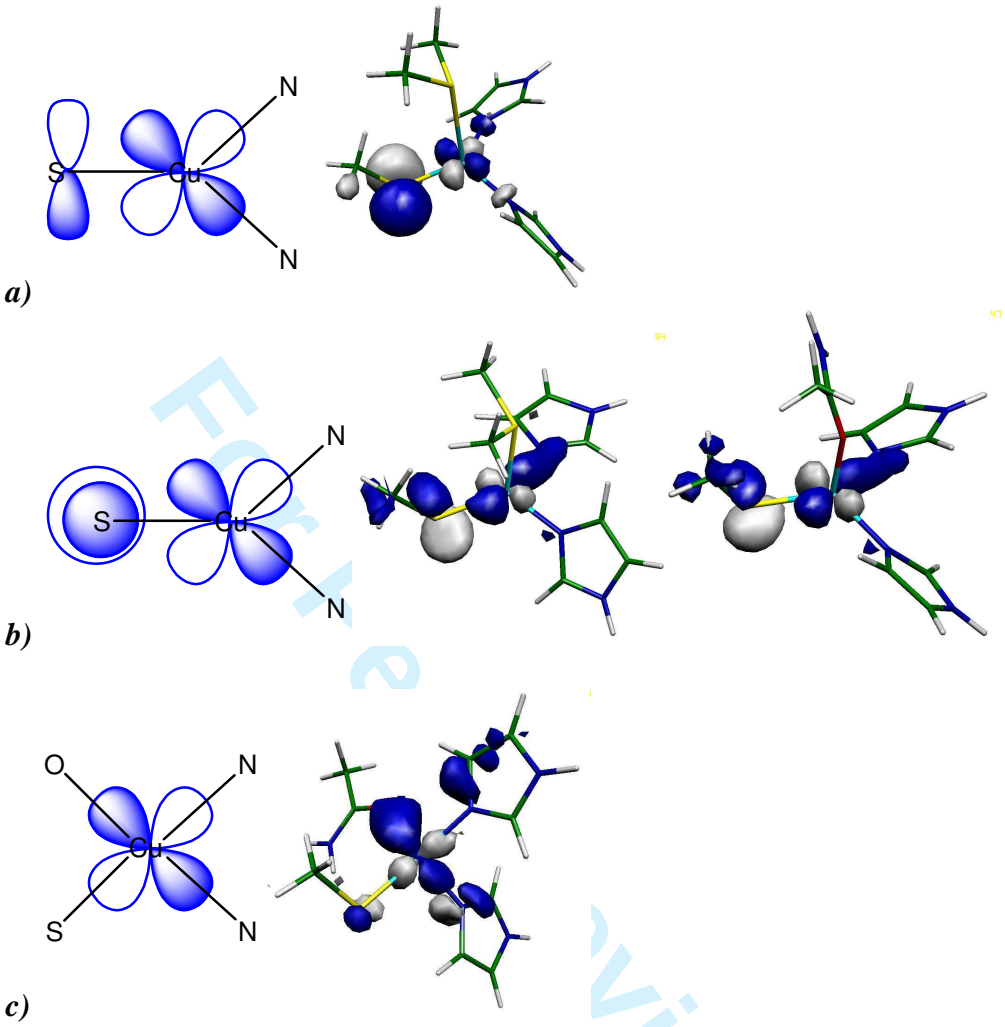

Figure 7